Published in "Macromolecules 41(9): 3243–3249, 2008"
which should be cited to refer to this work.

Direct Imaging of Nanoscopic Plastic Deformation below Bulk T_g and Chain Stretching in Temperature-Responsive Block Copolymer Hydrogels by Cryo-TEM

Antti Nykänen,[†] Markus Nuopponen,[‡] Panu Hiekkataipale,[†] Sami-Pekka Hirvonen,[‡] Antti Soininen,[†] Heikki Tenhu,[‡] Olli Ikkala,[†] Raffaele Mezzenga,[§,||] and Janne Ruokolainen*,[†]

Department of Engineering Physics and Center for New Materials, Helsinki University of Technology, P.O Box 5100, FI-02015 TKK, Finland; Department of Chemistry, University of Helsinki, P.O. Box 55, 00014 Helsinki, Finland; Department of Physics and Fribourg Center for Nanomaterials, University of Fribourg, Perolles Fribourg, CH-1700 Switzerland; and Nestlé Research Center, Vers-Chez-les-Blanc, 1000 Lausanne 26, Switzerland

ABSTRACT: This work describes the thermoresponsive transition in polystyrene-*block*-poly(*N*-isopropylacrylamide)-*block*-polystyrene (PS-*block*-PNIPAM-*block*-PS) triblock copolymer hydrogels, as observed by both direct and reciprocal space in-situ characterization. The hydrogel morphology was studied in both the dry and wet state, at temperatures below and beyond the coil−globule transition of PNIPAM, using vitrified ice cryo-transmission electron microscopy (cryo-TEM), in-situ freeze-drying technique, and small-angle X-ray scattering (SAXS). The selected PS-*block*-PNIPAM-*block*-PS triblock copolymers were intentionally designed in such a molecular architecture to self-assemble into spherical and bicontinuous morphology with the poly(*N*-isopropylacrylamide) forming the continuous matrix. The phase behavior in bulk was directly investigated by SAXS as a function of temperature, while free-standing polymer thin films of samples quenched from different temperatures, allowed observing by cryo-TEM the changes in hydrogel microstructure. Finally, sublimation of water via controlled freeze-drying in the TEM column allowed studying systems without the presence of vitrified water, which enables direct imaging of the densely connected physically cross-linked polymer network. By combining these techniques on samples exhibiting both spherical and gyroidal morphologies, it was demonstrated that (i) PNIPAM form physically connected networks in spherical structures and bicontinuous morphologies in the gyroidal phase, (ii) in PNIPAM chains strands are strongly stretched above the polymer coil-to-globule transition, and (iii) surprisingly, upon the gel swelling process, the PS domains undergo extensive plastic deformation although temperature is always maintained well below the PS glass transition bulk temperature. The possible physical mechanisms responsible for this plastic deformation can be understood in terms of the dependence of PS glass transition temperature on the size of nanometer-scaled domains.

Introduction

Poly(*N*-isopropylacrylamide) (PNIPAM) is one of the most extensively investigated synthetic temperature-responsive polymers.[1–4] In aqueous solutions it undergoes a reversible coil−globule transition at temperature of ca. 32 °C, and upon heating beyond this temperature, the changes in the PNIPAM chain conformation occur in a sharp manner, within a few degrees.[5] This property makes this polymer a very interesting building block for functional organic materials. One widely studied concept which exploits this transition is based on responsive polymer networks in water solutions, also commonly referred as "smart" hydrogels, since they can react in a specific way to the external environmental stimuli. Smart hydrogels are typically obtained by cross-linking the responsive polymers such as PNIPAM to form covalently bonded networks or interpenetrating network structures.[6–9] Alternatively, block copolymers containing a hydrophilic midblock and hydrophobic end blocks can also be used to form physically cross-linked systems with thermoresponsive behavior.[10,11] Hydrogels have also been designed by combining two types of polymers capable of interacting via mutual hydrogen bonding into interpenetrating networks[12,13] or by using water-soluble ABA triblock copolymers where the solubility of the end blocks is suitably controlled by external conditions.[14–17] Recently, also protein-based materials,[18–20] polypeptides,[21,22] and block copolypeptides[23–25] have been exploited to design stimuli-responsive gels. In our previous work we have demonstrated a simple way to form responsive polymer networks by using ABA triblock copolymers, which can self-assemble into spherical, cylindrical, lamellar, or double-gyroid morphologies.[26] By designing the triblock copolymer in such a way to maintain the responsive PNIPAM midblock in the continuous phase, these materials can be swollen by any selective solvent for the midblock. The temperature responsive behavior of various PS-*block*-PNIPAM-*block*-PS triblock copolymers gels in water was investigated in detail in our previous paper, by measuring volume expansion and weight pickup in wet environment or by studying the filtration properties of these materials with respect to hydrophilic polymers, below and above the coil−globule transition of the PNIPAM.[26]

Nonetheless, a few methods are available to probe directly the changes arising in the morphology of responsive polymers. Small-angle X-ray scattering can be used to explain the changes in stimuli-responsive structure in block copolymer gels in bulk.[11,27] For responsive micelles in solution, light scattering studies can provide information on the change of micelle size with varying environmental stimuli.[28,29] However, these methods give only statistically averaged information on the transition behavior, and they only provide information on the reciprocal space, so that models have often to be used in order to account

* Corresponding author: e-mail janne.ruokolainen@tkk.fi.
[†] Helsinki University of Technology.
[‡] University of Helsinki.
[§] University of Fribourg.
[||] Nestlé Research Center.

for morphology changes. In order to study morphological changes of responsive polymer systems in real space, microscopy methods such as laser scanning confocal microscopy,[22,30] atomic force microscopy equipped with environmental cell,[31,32] or cryo-electron microscopy (cryo-TEM) techniques[33–35] are required. Conventional electron microscopy methods operating in high-vacuum conditions require complete drying of the hydrogel sample or the use of chemical fixation, which results in manipulation and possible artifacts in the gel structure. In cryo-TEM the physical fixation of solution is achieved by rapidly plunging the liquid dispersion into a suitable cryogen to convert the liquid solvent into its glassy solid state.[33,36] As a consequence, samples swollen in vitrified solvent do not exhibit the artifacts that would normally occur when using chemical fixation or staining and drying techniques. Recently, Ballauff and co-workers used cryo-TEM to image volume transitions of thermoresponsive PS−PNIPAM core−shell particles, and they could elucidate new mechanisms about network thermal fluctuations which were not available previously using standard light or X-ray scattering investigations.[34]

In this work cryo-TEM has been used to characterize PS-*block*-PNIPAM-*block*-PS triblock copolymer hydrogels morphology in their native hydrated state. We report for the first time the stimuli-responsive behavior in thermoresponsive self-assembled block copolymer gels by combining the direct real-space cryo-TEM imaging with supporting experiments made by small-angle X-ray scattering measurements. Furthermore, by sublimating the vitrified water via a well-controlled in-situ freeze-drying method inside the transmission electron microscope, we have obtained direct information on (i) the stretching of PNIPAM polymer chains connecting PS spherical domains in spherical morphologies and the network structure and (ii) connectivity in gyroidal morphologies. Finally, we provide evidence that, in both spherical and gyroidal morphologies, the PS domains undergo extensive plastic deformation during the gel swelling process, although the temperature is always maintained well below the PS bulk glass transition temperatures. The reasons for this plastic behavior are discussed and argued in the last part of the paper.

Experimental Methods

Materials. Tetrahydrofuran (THF, 99%) was used as received from Fluka. Synthesis of PS-*block*-PNIPAM-*block*-PS triblock copolymers by controlled RAFT polymerization is described in our previous paper.[26] For this study two triblock copolymers were selected: sample PN77.118K with the total molecular weight of $M_n = 118\,300$ gmol^{-1}, polydispersity index $M_w/M_n = 1.51$, and PNIPAM weight percentage of 77 wt % and sample PN61.106K with $M_n = 106\,000$ g mol^{-1}, $M_w/M_n = 1.52$, and PNIPAM weight percentage of 61 wt %.

Small-Angle X-ray Scattering. Polymer was dissolved in THF to yield 1.0 wt % solution. The solvent was then evaporated from the solution at room temperature yielding the solid sample, which was further dried in vacuum at room temperature for 4−6 h. In order to obtain thermodynamically stable morphologies, the sample was annealed at ca. 180 °C under a high vacuum $p \approx 10^{-8}$ mbar for 3−4 days. The structural periodicities were measured by small-angle X-ray scattering using Bruker Microstar microfocus X-ray source with a rotating anode (Cu Kα radiation, $\lambda = 1.54$ Å) and with Montel Optics. The beam was further collimated with four sets of four-blade slits (JJ-X-ray), resulting in a beam of about 0.65 mm × 0.65 mm at the sample position. The distance between the sample and the 2D detector (Bruker AXS) was 3.5 m. The magnitude of the scattering vector is given by $q = (4\pi/\lambda) \sin \theta$, where 2θ is the scattering angle. Corrections for spatial distortion and detector response were made using a Fe-55 source. The SAXS patterns from the samples were absorption corrected, and the background scattering was subtracted.

Transmission Electron Microscopy (TEM). In order to avoid any possible artifact from the cryo-microtoming process, thin films were spin-coated on sodium chloride crystal substrates (Sigma Aldrich, FTIR window) by dropping 30 μL of 3 wt % THF solution of PS-*block*-PNIPAM-*block*-PS on the center of the substrate, which was spinning at a speed of 1000 rpm. The advantage of using sodium chloride crystal substrates is that, besides the fact that their surface is smooth, annealed films can be easily floated off them onto the water surface. This is not the case for other smooth surfaces such as Si. In cryo-TEM conventional staining methods are difficult to apply. Therefore, in order to increase contrast between the microphase-separated polymer domains, polystyrene coated gold nanoparticles were added to the polymer solution; however, the contrast was sufficient without any added nanoparticles. For the unstained samples polystyrene domains appear dark in the image due to higher electron density compared to PNIPAM matrix. The resulting film thickness was ∼250 nm, as measured by atomic force microscopy. Thin films were dried and annealed following the same procedure used for the bulk samples for X-ray analysis. In order to remove the sodium chloride substrate, annealed films were floated on 55 °C water, which is a nonsolvent for PNIPAM, and picked up on 600 mesh size copper grids.

Hydrogel thin films were swollen on grids by keeping the grids on 5 °C water at least 15 min, after which the grids were transferred into environmental chamber of Tecnai Vitrobot having relative air humidity of 100%. To remove all the residual water, three consecutive 1 s blottings were made followed by immediate plunging of the samples into liquid ethane at −175 °C. Experiments were carried out with environmental chamber temperatures of 5, 30, 35, and 45 °C. Vitrified samples were cryo-transferred into FEI Tecnai 12 transmission electron microscope using a Gatan 910 cryo-transfer holder, whose temperature was maintained at −185 °C. Samples were imaged by TEM operated at an acceleration voltage of 120 kV using bright field mode. We recorded micrographs using a Gatan UltraScan 1000 camera having a CCD size of 2048 × 2048 pixels. Moreover, in order to observe the network structure of the polymer film without the presence of vitrified ice within the PNIPAM matrix, water was allowed to sublimate (at pressure corresponding to the vacuum of the TEM column) by in-situ freeze-drying of the samples by increasing the cryo-sample holder temperature from −185 to −80 °C.

Atomic Force Microscopy (AFM). Polymer film thickness was measured using Digital Instrument Nanoscope III atomic force microscope using tapping mode. Crack was made by razor blade on polymer film spun on glass substrate, and thickness was measured from the topographic image scanned over the crack.

Results and Discussion

The block copolymers considered in this study are designed with a molecular architecture suitable for maintaining the PNIPAM block in the continuous matrix, while the polystyrene end-block chains are connected by either spherical or bicontinuous "gyroid" PS domains, thus providing the physical cross-links. Because of the temperature-dependent water solubility of the PNIPAM block, the hydrogel is expected to swell below the coil−globule transition temperature and to shrink beyond the temperature, as schematically illustrated in Figure 1.

Parts A and B of Figure 2 show the morphology for dry PS-*block*-PNIPAM-*block*-PS hydrogel samples with 77 and 61 wt % PNIPAM, respectively. For the unstained samples polystyrene domains appear dark in the image due to higher electron density compared to PNIPAM matrix. In the sample containing 77 wt % of PNIPAM the morphology is clearly spherical with average polystyrene sphere diameter of 20 nm. For the sample having 61 wt % PNIPAM the morphology cannot be unambiguously determined on the basis of TEM micrographs such as those presented in Figure 2B alone, but as it will be shown later by the cryo-TEM experiments carried out on swollen vitrified samples, the morphology can clearly be attributed to a gyroidal

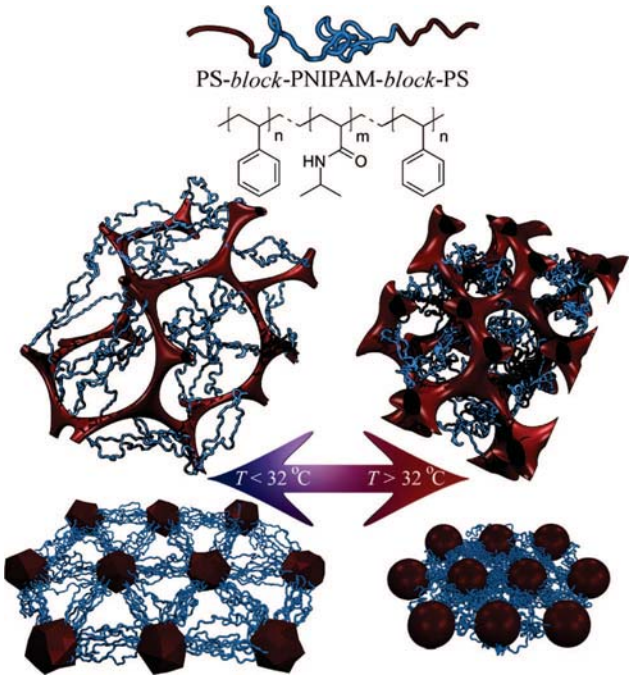

Figure 1. Chemical structure of polystyrene-*block*-poly(*N*-isopropylacrylamide)-*block*-polystyrene triblock copolymer and a schematic illustration of temperature-induced conformation transition of aqueous hydrogel having self-assembled morphologies with spherical or "gyroid" PS domains. In both cases, PS domains act as physical cross-links for the hydrogel.

structure. The morphologies reported in Figures 2A,B are in agreement with those previously observed by the authors in bulk systems.[26]

Use of cryo-TEM was made in order to directly observe the hydrogel thermoresponsive swelling behavior. As the water vitrification process is very rapid, the gel microstructure at the state defined by the environmental chamber conditions at which the samples were exposed and equilibrated prior to vitrification, is expected to be preserved. Thus, depending on the temperature of the chamber, both morphologies below and beyond the PNIPAM transition temperature could be observed. Figures 3A,B show cryo-TEM images taken from the sample having 77 wt % of PNIPAM and vitrified from below the coil-to-globule transition temperature (5 and 30 °C, respectively). At these temperatures the PNIPAM chains are hydrophilic and the water is diffusing into the film, swelling it. Above the coil-to-globule transition, PNIPAM chains become hydrophobic and water is expelled out of the film, leading to marked shrinkage of the structure. This is directly shown by the TEM micrographs presented in Figures 3C,D, taken from samples vitrified from 35 and 45 °C, respectively. Therefore, the increased distance between the polystyrene spheres in Figures 3A,B, compared to the distance observed in the dry film (Figure 2A) or in the film vitrified from 35 and 45 °C (Figures 3C,D), is the direct consequence of increased end-to-end distance in PNIPAM midblock chain as a consequence of the polymer coil−globule transition occurring at 32 °C.

In order to validate the presence of a physically cross-linked network in PS-*block*-PNIPAM-*block*-PS hydrogels as well as to investigate the topology and continuity of this network in thin film, water was allowed to sublimate from the vitrified samples via controlled freeze-drying by increasing temperature of the cryo-holder from −185 to −80 °C. While at −185 °C vitrified water can be maintained in this state at the high TEM vacuum, at −80 °C sublimation takes place, and only the dry polymer network forming the hydrogel is left over. Figure 4A shows the freeze-dried cryo-TEM micrograph of the hydrogel with spherical morphology vitrified from 45 °C, i.e., above the PNIPAM coil−globule transition temperature. As expected, the film structure does not change during the freeze-drying process, and spherical PS morphology in dense PNIPAM matrix is still observed. More importantly, the unaffected PS interparticle distance further confirms the absence of the water in the gel vitrified from above the coil−globule transition temperature.

A very different behavior, however, is revealed for the PS-*block*-PNIPAM-*block*-PS hydrogel with spherical morphology when this was vitrified from below the PNIPAM coil−globule transition temperature, as shown in Figure 4B. Drastic changes occur during the freeze-drying process as demonstrated by the final porous coarse meshed structure with a dense connectivity of the network formed by PNIPAM strands. A sparse network structure is indeed expected, since based on our previous bulk swelling studies, below 32 °C this sample swells approximately 35−40 times by the weight and contains therefore up to 95 wt % water.[26] The micrograph in Figure 4B also shows that, after freeze-drying water removal, the PNIPAM chains forming the strands are very stretched and that these strands physically connect the adjacent PS domains, as may typically be expected in a triblock copolymer spherical morphology.

The PNIPAM midblock end-to-end distance can be roughly estimated by measuring the PNIPAM strand lengths directly from TEM images taken from freeze-dried swollen network structures (such as that reported in Figure 4B). The measured PNIPAM strand lengths are typically in the range of up to 100−150 nm. It should, however, be borne in mind that TEM images represent a two-dimensional projection of a randomly oriented 3D structure and that as a consequence only the longest distances measured from the TEM images correspond the real distances between the PS spheres. The fully extended chain length (contour length) of the PNIPAM midblock can be estimated from its molecular weight, which for the sample considered in Figure 4 is 90 kg/mol and equals about 800 NIPAM monomers. By taking the typical C−C bond length of 1.5 Å and bond angle of 110°, the PNIPAM midblock contour length is estimated to be ∼200 nm. Therefore, in a swollen hydrogel network PNIPAM end-to-end distances are close to the PNIPAM contour length, indicating that the chains are so highly stretched to be close to fully extended configuration. It can consequently be argued that it is the limit in the stretching of PNIPAM chains which settles the maximum amount of water pickup by the triblock hydrogels. This rough argument, to be corrected by the entropy loss of highly stretched chains, can be used as a rational to understand the differences in water pickup by different hydrogel structures.[26]

In order to investigate further the role of self-assembled block copolymer bulk morphologies on the topology of PS-*block*-PNIPAM-*block*-PS physically cross-linked hydrogels, sample PN61.106K with 61 wt % PNIPAM was investigated following the same cryo-TEM and freeze-drying procedures used for sample PN77.118K.

Figure 5A shows a cryo-TEM image of the freeze-dried sample PN61.106K vitrified from the hydrogel swollen state (T = 5 °C). This sample is expected to have bicontinuous morphology in thin film before the swelling.[26] The micrograph clearly demonstrates that the bicontinuous structure is present, and it is preserved during the process of hydrogel swelling and freeze-drying. Polystyrene, appearing dark in the micrographs, forms a continuous network throughout the swollen hydrogel, and both 3-fold and 4-fold symmetries can be recognized in many junction points, as it can be more clearly seen in higher magnification image (Figure 5B). For block copolymers in bulk having double-gyroid morphology, 3-fold symmetry can be observed by TEM in images taken from the [111] lattice

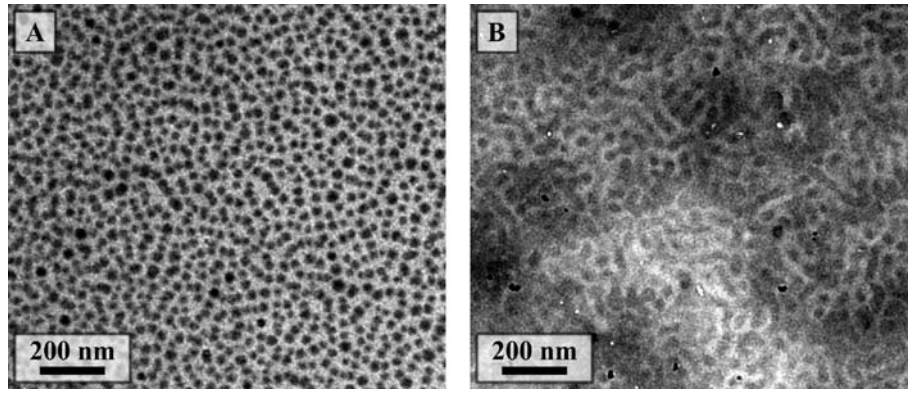

Figure 2. Representative TEM micrographs of dry PS-*block*-PNIPAM-*block*-PS triblock copolymer thin films with spherical and bicontinuous morphology: (A) sample PN77.118K with 77 wt % PNIPAM and (B) sample PN61.106K with 61 wt % PNIPAM.

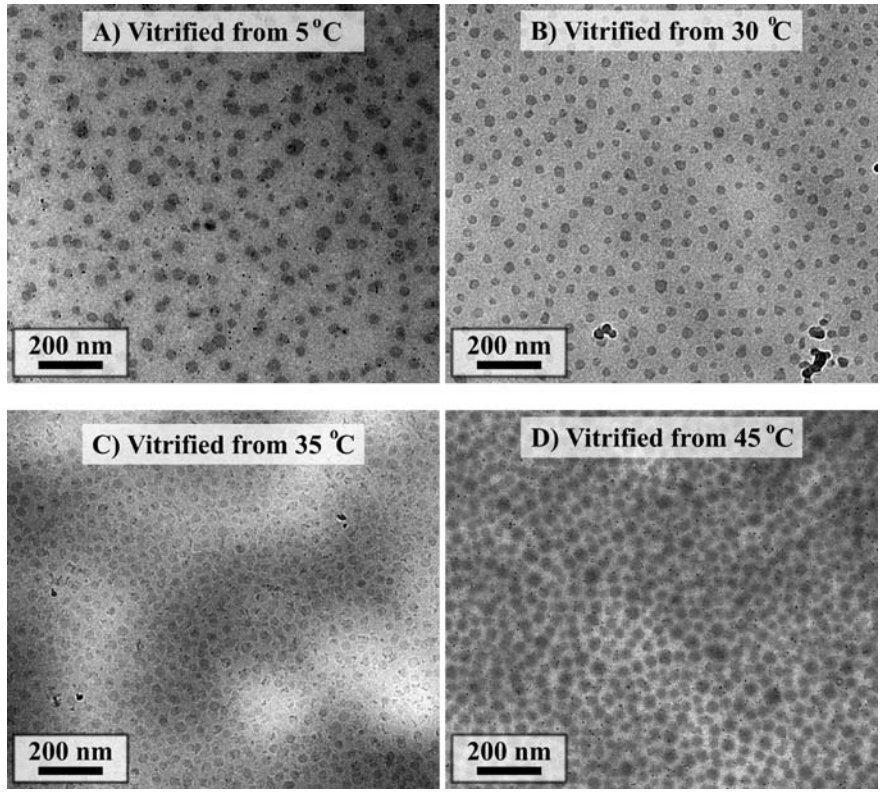

Figure 3. Cryo-TEM micrographs of PS-*block*-PNIPAM-*block*-PS block copolymer hydrogel sample PN77.118K xposed to water: (A) vitrified from 5 °C and 100% humidity; (B) vitrified from 30 °C and 100% humidity; (C) vitrified from 35 °C and 100% humidity; (D) vitrified from 45 °C and 100% humidity. A sharp transition in the distance between the polystyrene spheres occurs between 30 and 35 °C.

projection, while 4-fold symmetry may appear in [100] projection images.[37–39] Therefore, these images clearly support our previous attribution of this sample to a bicontinuous double-gyroid morphology.[26] In bulk this sample swells approximately 7−10 times by weight which corresponds well with the observed changes in the microstructure length scale in the cryo-TEM images. Indeed, before swelling the "mesh size" is ∼45 nm (Figure 2B), while after the swelling the average domain size is 80−100 nm (Figure 5B), which is roughly the change expected on the basis of volume swelling considerations.

Interestingly, continuous "gyroid" polystyrene skeleton is well preserved and is not disrupted during the hydrogel swelling process. However, before swelling the polystyrene domain average diameters are ∼20 nm (Figure 2B) while after swelling the polystyrene domains have undergone a severe plastic deformation, with strongly stretched strands and much smaller diameter, typically below 10 nm. Careful analysis of the other cryo-TEM images acquired for PN77.118K sample revealed that also in the case of spherical morphologies polystyrene domains are plastically deformed during the swelling process. Figure 6 illustrates the plastic deformation of polystyrene domains for PN77.118K from spherical to polyhedral shapes, appearing as pentagon-like or triangular-like depending on TEM projection, as highlighted by the arrows. Because such plastic deformation can be observed also in vitrified samples prior to freeze-drying process (not shown here), deformation of PS domains as an artifact due to the freeze-drying process can be ruled out, in favor of a real physical process occurring during the hydrogel swelling process. Presumably, the PNIPAM strands apply a pulling pressure on the PS domains which can either deform the PS spheres into polyhedrons or the PS gyroidal strands into thinner and longer strands. Previously, similar plastic deformations from sphere-to-polyhedron have been reported for PS colloidal particles blended with block copolymers exerting a pulling packing frustration profile on the colloidal surface.[40] However, the results presented in the present study are

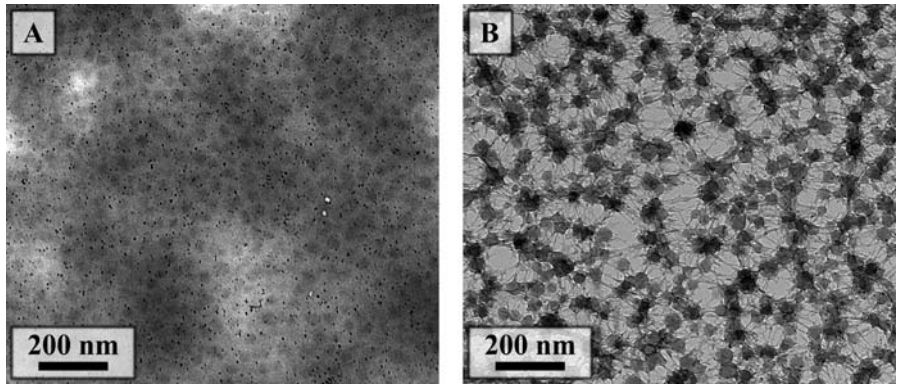

Figure 4. In-situ freeze-dried cryo-TEM micrograph of PS-*block*-PNIPAM-*block*-PS block copolymer hydrogel sample PN77.118K exposed to water: (A) sample vitrified from 45 °C; (B) sample vitrified from 5 °C.

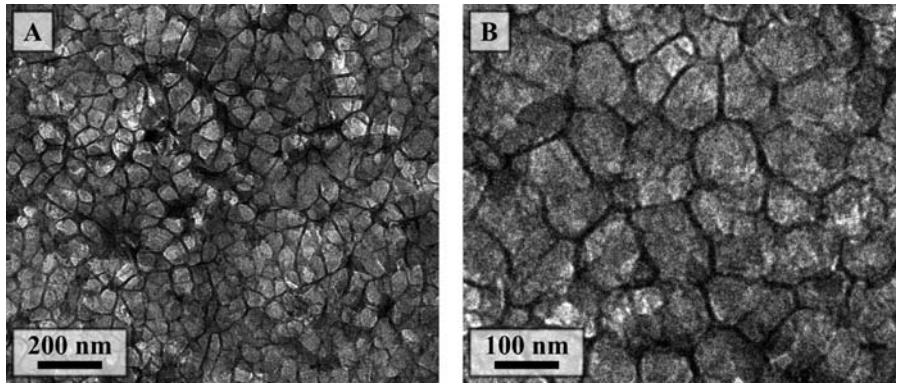

Figure 5. (A) Cryo-TEM images of sample PN61.106K having bicontinuous morphology. Sample is vitrified from the swollen hydrogel state (T = 5 °C) followed by in situ freeze-drying at −80 °C. (B) Higher magnification clearly reveals the continuous plastically deformed polystyrene network with 3-fold and 4-fold symmetry in the junction points.

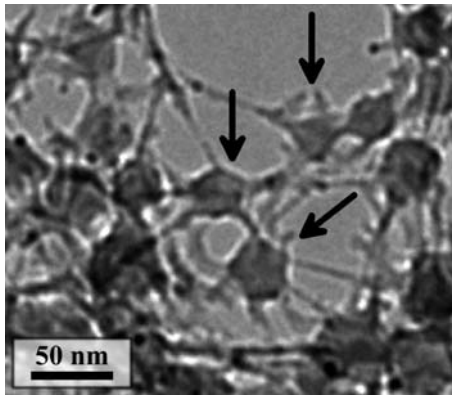

Figure 6. High-magnification freeze-dried cryo-TEM micrograph of the PN77.118K sample with spherical morphology. Sample is vitrified from the swollen hydrogel state (T = 5 °C). Arrows highlight the polystyrene spheres which have transformed into polyhedrons (with pentagonal or triangular projections in the TEM image) by extensive plastic deformation.

substantially different since, unlike those reported in ref 40 in which the plastic deformation takes place above the glass transition temperature (T_g) of bulk PS (∼100 °C); here, the swelling of both spherical and gyroidal hydrogels occurs at 5 °C, which is well below the T_g of bulk polystyrene.

Thus, it must be admitted that the T_g of PS microphase-separated domains is close to or below 5 °C. This can be explained by the fact that (i) the size of the polystyrene domains is relatively small, below 20 nm, and (ii) the molecular weight of the PS end blocks is rather low, ∼14 kg/mol for PN77.118K and 20 kg/mol for PN61.106K, which compares with or is slightly larger than the polystyrene entanglement molecular weight (M_e = 13.3 kg/mol).[41] Because bulk polystyrene with molecular weight of or beyond 15 kg/mol is generally behaving as glassy, we believe that the PS size domain argument better explains the observed plastic deformations. Moreover, since both the experimental and theoretical studies on the size-dependent T_g of PS ultrathin films have been already reported[42–44] and the significant sudden decrease of T_g below 100 nm scale has been suggested, the present results provide an important experimental confirmation of those previous findings.[42–44]

Small-angle X-ray scattering was employed to obtain more precise information concerning the characteristic length scales of the bulk hydrogel samples. Temperature-dependent SAXS diffractograms were acquired first on dry bulk samples and then on samples swelled with water at 20 °C, which is below the coil−globule transition of PNIPAM. For wet samples, temperature was varied upon heating, and diffractograms were acquired every 5 °C and collected as shown in Figure 7.

For the dry sample PN77.118K, a single-peak diffractogram with first-order peak at q = 0.0155 Å^{-1}, corresponding to 41 nm in characteristic length scale, was obtained, which is consistent with a poorly ordered spherical block copolymer morphology such as that reported in Figure 2A. After swelling the sample with water at 20 °C, the scattering peak is shifted to very small angles, with the first-order peak position measured at q = 0.0063 Å^{-1}, corresponding approximately to a 100 nm length scale in real space, which is again in agreement with PS interparticle distances observed by cryo-TEM for swelled sample PN77.118K (see Figures 3A,B). During the heating process from 20 °C upward, the first-order peak position shifts gently to higher angles, indicating onset of PNIPAM chains contractions, and at 30 °C, which is just below the PNIPAM transition temperature, the peak position is at 0.0073 Å^{-1}, corresponding to a

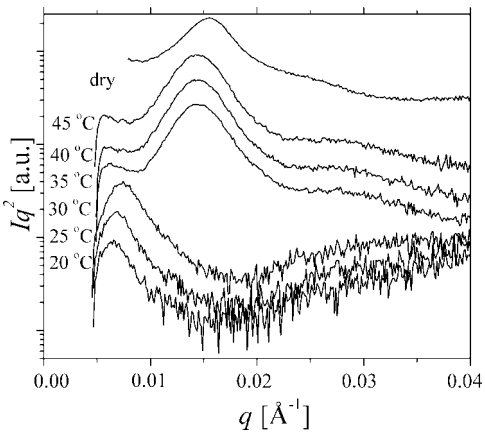

Figure 7. Small-angle X-ray scattering diffractograms of PN77.118K. Dry bulk sample at room temperature and for the hydrogel−water mixture collected after swelling upon heating from 20 to 45 °C measuring every 5 °C. Data show a very sharp structural transition at the PNIPAM coil-to-globule transition temperature, which occurs between 30 and 35 °C.

real space length scale of 86 nm. At the PNIPAM coil-to-globule transition temperature, which occurs between 30 and 35 °C, the peak suddenly shifts to high q values, and the peak position measured for the collapsed bulk above the transition temperature is practically the same as that measured for the dry bulk. Thus, in summary, the observed changes in the microstructure characteristic size agree well with both those observed by cryo-TEM studies and those expected on the basis of volume changes considerations.[26]

Conclusions

We have presented the first cryo-transmission electron microscopy study of self-assembled polystyrene-*block*-poly(*N*-isopropylacrylamide)-*block*-polystyrene triblock copolymer hydrogels at different temperature conditions. Cryo-TEM studies were supported by small-angle X-ray scattering analysis, while sublimation of vitrified water in hydrogel−water blends by in-situ freeze-drying in the transmission electron microscope column revealed detailed and valuable information about the hydrogel network structure, connectivity, and topology.

Two different polystyrene-*block*-poly(*N*-isopropylacrylamide)-*block*-polystyrene triblock copolymer hydrogels having a spherical and bicontinuous double-gyroidal microstructure were studied. The typical length scales observed for block copolymer microstructures by cryo-TEM on samples vitrified above and below the PNIPAM transition temperature compare well with the corresponding small-angle X-ray analysis and with expectations based on macroscopic gel swelling considerations. Additionally, besides providing direct verification of the spherical and double-gyroidal structure of the two hydrogels, the cryo-TEM analysis combined with freeze-drying process allowed gaining a deeper understanding and new valuable information about PNIPAM network microstructural deformation during the hydrogel swelling process. It was then demonstrated that in both spherical and gyroidal morphologies the polystyrene domains undergo severe plastic deformation during the hydrogel swelling, although the whole process occurs at temperatures well below the glass transition temperature of bulk polystyrene. This allowed arguing that confined polystyrene domains in these block copolymer systems have an effective glass transition temperature of 5 °C or less. The physical reasons for such an effective low glass transition temperatures were identified on the confinement of polystyrene domains within sizes less than 20 nm, which has profound effects on the glass transition temperature of PS, as already reported in the literature by other authors.

Acknowledgment. This work was carried out in the Centre of Excellence of Finnish Academy ("Bio- and Nanopolymers Research Group", 77317). Work was supported by the Finnish Funding Agency for Technology and Innovation (HUMA project), Finnish Academy, Finnish Cultural Foundation, National Graduate School in Material Physics, and Swiss Science National Foundation (SNF). This work made use of Helsinki University of Technology, Nanomicroscopy Center (TKK-Nmc) Facilities.

References and Notes

(1) Rzaev, Z. M. O.; Dincer, S.; Piskin, E. *Prog. Polym. Sci.* **2007**, *32* (5), 534–595.
(2) Schild, H. G. *Prog. Polym. Sci.* **1992**, *17* (2), 163–249.
(3) Pelton, R. *Adv. Colloid Interface Sci.* **2000**, *85* (1), 1–33.
(4) Nayak, S.; Lyon, L. A. *Angew. Chem., Int. Ed.* **2005**, *44* (47), 7686–7708.
(5) Fujishige, S.; Kubota, K.; Ando, I. *J. Phys. Chem.* **1989**, *93* (8), 3311–3313.
(6) Kaneko, Y.; Nakamura, S.; Sakai, K.; Aoyagi, T.; Kikuchi, A.; Sakurai, Y.; Okano, T. *Macromolecules* **1998**, *31* (18), 6099–6105.
(7) Zhang, J.; Peppas, N. A. *Macromolecules* **2000**, *33* (1), 102–107.
(8) Gutowska, A.; Bae, Y. H.; Jacobs, H.; Feijen, J.; Kim, S. W. *Macromolecules* **1994**, *27* (15), 4167–4175.
(9) Kuckling, D.; Harmon, M. E.; Frank, C. W. *Macromolecules* **2002**, *35* (16), 6377–6383.
(10) Ryan, A. J.; Crook, C. J.; Howse, J. R.; Topham, P.; Geoghegan, M.; Martin, S. J.; Parnell, A. J.; Ruiz-Perez, L.; Jones, R. A. L. *J. Macromol. Sci., Phys.* **2005**, *B44* (6), 1103–1121.
(11) Ryan, A. J.; Crook, C. J.; Howse, J. R.; Topham, P.; Jones, R. A. L.; Geoghegan, M.; Parnell, A. J.; Ruiz-Perez, L.; Martin, S. J.; Cadby, A.; Menelle, A.; Webster, J. R. P.; Gleeson, A. J.; Bras, W. *Faraday Discuss.* **2005**, *128*, 55–74.
(12) Bell, C. L.; Peppas, N. A. *Biopolymers II* **1995**, *122*, 125–175.
(13) Mathur, A. M.; Hammonds, K. F.; Klier, J.; Scranton, A. B. *J. Controlled Release* **1998**, *54* (2), 177–184.
(14) Fujiwara, T.; Mukose, T.; Yamaoka, T.; Yamane, H.; Sakurai, S.; Kimura, Y. *Macromol. Biosci.* **2001**, *1* (5), 204–208.
(15) Li, C. M.; Tang, Y. Q.; Armes, S. P.; Morris, C. J.; Rose, S. F.; Lloyd, A. W.; Lewis, A. L. *Biomacromolecules* **2005**, *6* (2), 994–999.
(16) Mukose, T.; Fujiwara, T.; Nakano, J.; Taniguchi, I.; Miyamoto, M.; Kimura, Y.; Teraoka, I.; Lee, C. W. *Macromol. Biosci.* **2004**, *4* (3), 361–367.
(17) Yoshida, T.; Kanaoka, S.; Watanabe, H.; Aoshima, S. *J. Polym. Sci., Part A: Polym. Chem.* **2005**, *43* (13), 2712–2722.
(18) Petka, W. A.; Harden, J. L.; McGrath, K. P.; Wirtz, D.; Tirrell, D. A. *Science* **1998**, *281* (5375), 389–392.
(19) Kulkarni, S.; Schilli, C.; Grin, B.; Muller, A. H. E.; Hoffman, A. S.; Stayton, P. S. *Biomacromolecules* **2006**, *7* (10), 2736–2741.
(20) Stevens, M. M.; Allen, S.; Davies, M. C.; Roberts, C. J.; Sakata, J. K.; Tendler, S. J. B.; Tirrell, D. A.; Williams, P. M. *Biomacromolecules* **2005**, *6* (3), 1266–1271.
(21) Pochan, D. J.; Schneider, J. P.; Kretsinger, J.; Ozbas, B.; Rajagopal, K.; Haines, L. *J. Am. Chem. Soc.* **2003**, *125* (39), 11802–11803.
(22) Schneider, J. P.; Pochan, D. J.; Ozbas, B.; Rajagopal, K.; Pakstis, L.; Kretsinger, J. *J. Am. Chem. Soc.* **2002**, *124* (50), 15030–15037.
(23) Breedveld, V.; Nowak, A. P.; Sato, J.; Deming, T. J.; Pine, D. J. *Macromolecules* **2004**, *37* (10), 3943–3953.
(24) Nowak, A. P.; Breedveld, V.; Pakstis, L.; Ozbas, B.; Pine, D. J.; Pochan, D.; Deming, T. J. *Nature (London)* **2002**, *417* (6887), 424–428.
(25) Nowak, A. P.; Sato, J.; Breedveld, V.; Deming, T. J. *Supramol. Chem.* **2006**, *18* (5), 423–427.
(26) Nykänen, A.; Nuopponen, M.; Laukkanen, A.; Hirvonen, S. P.; Rytelä, M.; Turunen, O.; Tenhu, H.; Mezzenga, R.; Ikkala, O.; Ruokolainen, J. *Macromolecules* **2007**, *40* (16), 5827–5834.
(27) Howse, J. R.; Topham, P.; Crook, C. J.; Gleeson, A. J.; Bras, W.; Jones, R. A. L.; Ryan, A. J. *Nano Lett.* **2006**, *6* (1), 73–77.
(28) Zhou, X. C.; Ye, X. D.; Zhang, G. Z. *J. Phys. Chem. B* **2007**, *111* (19), 5111–5115.
(29) Nuopponen, M.; Ojala, J.; Tenhu, H. *Polymer* **2004**, *45* (11), 3643–3650.
(30) Pochan, D. J.; Pakstis, L.; Ozbas, B.; Nowak, A. P.; Deming, T. J. *Macromolecules* **2002**, *35* (14), 5358–5360.
(31) Sorrell, C. D.; Lyon, L. A. *J. Phys. Chem. B* **2007**, *111* (16), 4060–4066.

(32) Wiedemair, J.; Serpe, M. J.; Kim, J.; Masson, J. F.; Lyon, L. A.; Mizaikoff, B.; Kranz, C. *Langmuir* **2007**, *23* (1), 130–137.
(33) Cui, H.; Hodgdon, T. K.; Kaler, E. W.; Abezgauz, L.; Danino, D.; Lubovsky, M.; Talmon, Y.; Pochan, D. J. *Soft Matter* **2007**, *3* (8), 945–955.
(34) Crassous, J. J.; Ballauff, M.; Drechsler, M.; Schmidt, J.; Talmon, Y. *Langmuir* **2006**, *22* (6), 2403–2406.
(35) Estroff, L. A.; Leiserowitz, L.; Addadi, L.; Weiner, S.; Hamilton, A. D. *Adv. Mater.* **2003**, *15* (1), 38++.
(36) Dubochet, J.; Adrian, M.; Chang, J. J.; Homo, J. C.; Lepault, J.; McDowall, A. W.; Schultz, P. *Q. Rev. Biophys.* **1988**, *21* (2), 129–228.
(37) Forster, S.; Khandpur, A. K.; Zhao, J.; Bates, F. S.; Hamley, I. W.; Ryan, A. J.; Bras, W. *Macromolecules* **1994**, *27* (23), 6922–6935.
(38) Hajduk, D. A.; Harper, P. E.; Gruner, S. M.; Honeker, C. C.; Kim, G.; Thomas, E. L.; Fetters, L. J. *Macromolecules* **1994**, *27* (15), 4063–4075.
(39) Matsen, M. W. *J. Chem. Phys.* **1998**, *108* (2), 785–796.
(40) Mezzenga, R.; Ruokolainen, J.; Hexemer, A. *Langmuir* **2003**, *19* (20), 8144–8147.
(41) Fetters, L. J.; Lohse, D. J.; Richter, D.; Witten, T. A.; Zirkel, A. *Macromolecules* **1994**, *27* (17), 4639–4647.
(42) Forrest, J. A.; Dalnoki-Veress, K.; Stevens, J. R.; Dutcher, J. R. *Phys. Rev. Lett.* **1996**, *77*, 2002.
(43) Forrest, J. A.; Dalnoki-Veress, K. *Adv. Colloid Interface Sci.* **2001**, *94*, 167.
(44) Jiang, Q.; Lang, X. Y. *Macromol. Rapid Commun.* **2004**, *25*, 825.